



Contents list available at IJRED website

International Journal of Renewable Energy Development

Journal homepage: <https://ijred.undip.ac.id>



Research Article

Ultrathin Film Amorphous Silicon Solar Cell Performance using Rigorous Coupled Wave Analysis Method

Raghvendra Sarvjeet Dubey and Sigamani Saravanan*

Advanced Research Laboratory for Nanomaterials & Devices, Department of Nanotechnology, Swarnandhra College of Engineering & Technology, Seetharampuram, Narsapur-534280, West Godavari (AP), India

Abstract. The issues related to global energy needs and environmental safeties as well as health crisis are some of the major challenges faced by the human, which make us to generate new pollution-free and sustainable energy sources. For that the optical functional nanostructures can be manipulated the confined light at the nanoscale level. These characteristics are emerging and leading candidate for the solar energy conversion. The combination of photonic (dielectric) and plasmonic (metallic) nanostructures are responsible for the development of better optical performance in solar cells. Here, the enhancement of light trapping within the thin active region is the primary goal. In this work, we have studied the influence of front-ITO (rectangular) and back-Ag (triangular) nanogratings were incorporated with ultrathin film amorphous silicon (a-Si) solar cell by using rigorous coupled wave analysis (RCWA) method. The improvement of light absorption, scattering (large angle), diffraction and field distributions (TE/TM) were demonstrated by the addition of single and dual nanogratings structures. Significantly, the plasmonic (noble metal) nanogratings are located at the bottom of the cell structure as a backside reflector which is helpful for the omni-directional reflection and increased the path length (life time) of the photons due to that the collection of the charge carriers were enhanced. Further, the proposed solar cell structure has optimized and compared to a back-Ag, front-ITO and dual nanogratings based ultrathin film amorphous silicon solar cell. Finally, the obtained results were evidenced for the assistance of photonic and plasmonic modes and achieved the highest current density (J_{sc}) of 23.82 mA/cm² (TE) and 22.75 mA/cm² (TM) with in 50 nm thin active layers by integration of (dual) cell structures.

Keywords: Light-trapping, solar cell, ultrathin film, plasmonic, RCWA



@ The author(s). Published by CBIORE. This is an open access article under the CC BY-SA license (<http://creativecommons.org/licenses/by-sa/4.0/>).

Received: 8th April 2022; Revised: 11th May 2022; Accepted: 20th May 2022; Available online: 29th May 2022

1. Introduction

In the quest of alternative renewable energy sources, thin film solar cell technology seems to be a promising due to the unlimited amount of energy source from the sun. The field of photonics and plasmonics has been propelled greatly in various applications like solar cell, antenna etc (Tran *et al.*, 2020; Schuller *et al.*, 2010; Belhadji, 2022; Hamdani *et al.*, 2022). Last few decades, solar cell technology has been developed and still an expensive as compared to the fossil fuels. In order to reduce the cost with enhanced performance, silicon is the best candidates. Particularly, amorphous silicon is a very attractive material and leading on the photovoltaic market due to their enhanced charge carrier mobility in the visible spectral region. However, thin film technology generates the hampered performance due to their lower cell efficiency in the visible and near-infrared spectral region. Further, the noble metallic (Au, Ag, and Cu) nanostructures can address this issue by controlling over the geometry at nanoscale level (Gong and Leite, 2016; Prabhakar, 2019). Among these nanostructures, silver (Ag) has less parasitic loss as reported by various researchers. For that Ag and Au materials are widely used in solar cells

for strong light scattering and improved light absorption in the visible spectral ($\lambda=380-700$ nm) region as reported by Pillai and Green (2010). Similarly, the ultraviolet and visible spectrum absorbed by copper (Cu) and aluminum (Al) nanostructures as demonstrated by Catchpole and Polman (2008). The different incident light (wavelength) can strongly improve light trapping in the matter by the way of strong confinement of light (interaction) and increasing optical (charge carrier) path length. To enhance the electron-hole pair path length, the collection (concentration) of photon should be increased within the thin active (absorber) layer regions. For that the active layer thickness must be lesser than the light exciton wavelength (diffused) as reported by various researchers (Khai *et al.*, 2011; Agrawal *et al.*, 2008). Nowadays, an ultrathin solar cells have been attractive for the low-cost, easy fabrication (small-scale) and novel conversion mechanisms. Various solar cell designs were proposed and provided remarkable optical performance enhancement through photonic crystals. Phengdaam *et al.*, (2021) experimentally investigated by the incorporation of mixed (red, purple, and blue) silver nanoprisms with the hole-transport layer of organic solar cells with the excitement of

*Corresponding author
Email: shasa86@gmail.com (S. Saravanan)

multiple placements which was helped to induce the broader light absorption. These silver nanoprisms sizes were 100 nm and achieved 7.9% cell efficiency using finite-difference time-domain (FDTD) method. Singh *et al.*, (2010) presented a thin film GaAs solar cell performance with metal nanoparticles (Ag, Al, Cu and Au) using FDTD method. Among the various metallic nanoparticles, the strong plasmonic scattering effect noticed with an optimized period of 100 nm and 40 nm radius. The optimized GaAs thin film solar cell showed the relative enhancement of current density up to 31% as compared reference cell. Saadman *et al.*, (2020) synthesized silver nanoparticles (with TiO₂) and used as fortunate in dye-sensitized solar cells (DSSCs) to enhance the optical performance. This demonstrated photovoltaic structure highly yielded 1.76% cell efficiency as compared to the reference DSSC (0.98%) without silver nanoparticles. Chriki *et al.*, (2013) proposed an ultrathin film silicon solar cell with dual plasmonic grating structures by using FDTD and rigorous coupled wave analysis (RCWA) methods. They found the highest current density (J_{sc}) enhancements of 1.86 under air mass 1.5G. Further, the influence of ITO-conductive oxide and Ag-metallic grating nanostructures performance was compared. Chen *et al.*, (2012) proposed a broadband light absorption with silver nanoparticles integrated thin film amorphous silicon (a-Si) solar cells. These silver nanoparticles were prepared by industry-friendly wet chemical method. They achieved 23% current density enhancement and 8.1% of cell efficiency. Saravanan and Dubey (2021) proposed ultrathin film amorphous silicon solar cell performance with the assistance of photonic and plasmonic modes by using RCWA method. They achieved the highest current density of 33.52 mA/cm² (transverse magnetic mode) within 390 nm cell thickness due to the integration of photonic (SiO₂) and plasmonic (Ag) nanogratings structures. Our proposed work, we are investigating the influence of front-ITO (rectangular) and rear-Ag metallic (triangular) nanogratings within 50 nm amorphous silicon active regions. In this designed cell, the plasmonic modes are dominated and received the highest current density of 23.82 mA/cm² in the transverse electric (TE) polarizations. First, the formation of top-ITO dielectric gratings embedded in the active region, whereas the second mechanism includes bottom triangular-Ag nanogratings directly into the active layer. Finally, third one consists of dual gratings (top & bottom gratings) on the backside reflectors. Because, photonic and plasmonic nanostructures are having enough number of photon and plasmon to reach a certain place in solar cells. Further, the light harvesting or distribution evidenced for improved thin film amorphous silicon solar cells.

2. Designing Approach

2.1 RCWA Method

A careful solar cell design is crucial for the optimizing optical performance in thin film solar cells. The schematic diagram of our proposed ultrathin amorphous silicon solar cell structure is shown in Figure 1. In the simulation (one-dimensional) process, the proposed design consists of the computational domain are periodic boundary conditions (PBC) in X- and Y-coordination axis (left and right) and perfectly matched layer (PML) in the Z- axis (top and bottom). Initially, the silver used as a substrate and top of

that the amorphous silicon active layer placed. The triangular metallic-Ag nanogratings positioned at the bottom of the active regions for improving light scattering, and diffraction which is helpful for the enhanced light absorption. This enhancement of light trapping evidenced in the transverse electric (TE) and magnetic (TM) field distribution as shown in Figure 4. Here, the addition of metallic nanostructures is decreasing the amount of active materials which helps to attain high solar cell performance (Prabhakar Rai, 2019). Next, ITO materials considered as an anti-reflection coating layer and front nanogratings (rectangular) which is reducing the light reflectance and shorter (ultraviolet and near visible) spectrum lights are efficiently spreading into the active region. After reaching the backside reflector, the incidence light (or wave) has scattered at omnidirectional way on top of the metallic-Ag back reflector surface which supports improved the light absorption in thin film solar cells (Shi *et al.*, 2013).

2.2 Current Density (J_{sc}) and light absorption

The characteristic equation for the calculation of current density (J_{sc}) can be expressed as follows,

$$J_{sc} = \frac{e}{hc} \int_{300}^{1200} \lambda A(\lambda) \frac{dI}{d\lambda} d\lambda \quad (1)$$

Where, 'e' elementary charge (4.355x10⁻¹⁹ coulombs), incident solar spectrum range considered from 300 (λ_1) to 1200 nm (λ_2), ' λ ' is the wavelength, 'c' is the speed of light in vacuum (2.99 x 10⁸ m/s), 'h' is the plank's constant (6.626 x 10⁻³⁴ Js), 'A' is the absorption within the amorphous silicon active region, and 'I' is the total incident spectrum (Wm⁻²nm⁻¹) (Saravanan *et al.*, 2015; Meng *et al.*, 2012). Furthermore, the total incident light absorption (A) can be calculated by using the following formula as,

$$A(\lambda) = 1 - R(\lambda) - T(\lambda) \quad (2)$$

Where, ' λ ' is the wavelength, 'R' reflectance and 'T' is the transmittance of the proposed solar cell (Prabhakar Rai, 2019). This investigation carried out by using the soft synopsis tool.

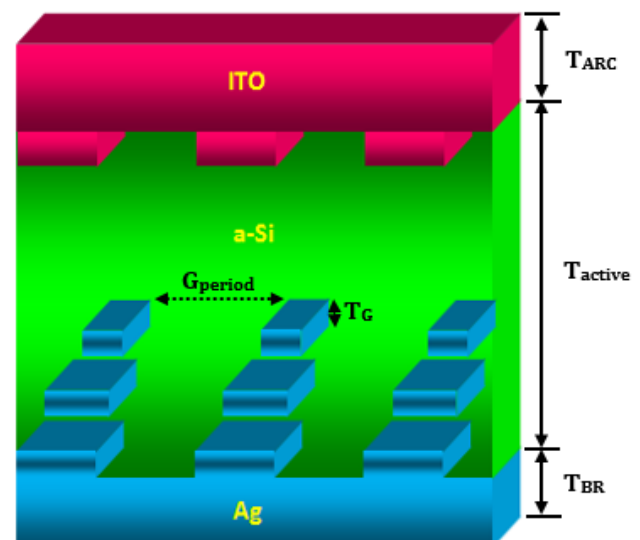


Fig. 1 The schematic diagram of thin film amorphous silicon solar cell.

Table 1

The list of materials refractive index, thickness and extinction coefficient.

Materials	Thickness D (nm)	Refractive index (n)	Extinction coeff. (k)
ITO	109	1.85	0.058
Front-ITO rectangular nanogratings	20	1.85	0.058
Amorphous Silicon	50	4.4	0.243
Rear-Ag triangular nanogratings	60	0.15	3.985
Ag Substrate	100	0.15	3.985

As per the literature survey, we have considered the amorphous silicon active layer due to their availability (non-crystalline form of silicon), high refractive index, experimentally feasible (plasma-enhanced chemical vapor deposition, PECVD) and significantly improved the optical performance. Further, the metallic grating can be fabricated by using various techniques such as epitaxial lift-off, RF sputtering, an etching method. Using PECVD, the amorphous silicon thin film can be grown and diffraction grating fabricated by sputtering/evaporation with dry/wet etching methods. The fabricated grating structure adhered on substrates (glass/silicon/steel/plastic film) and separated by electrochemical etching (or mechanical force) techniques. Next, the detached gratings with desired level (thickness) integrated by diffusion (or implantation) technique. Finally, the anti-reflection coating can be deposited by PECVD method and electrical contact provided for the testing.

The light path length of the photons enhanced due to the nanogratings integrated back reflector. Further, taking into the consistency of cell structure, the geometric parameters like the thickness (or height) of the each layer, the refractive indices of the materials and extinction coefficients were tabulated (Table-1). This entire design and simulation process was carried out by using rigorous coupled wave analysis method. This is a semi analytical technique also known as a Fourier model method. This rigorous coupled wave analysis, modeling method solver for Maxwell's equations and involves incident plane wave source. So, the complex solar cell design has optimized. It is important to maintain the cell thickness as less as possible for the photon path length enhancement in the solar cell with optimized light trapping mechanisms. In this aspect, the proposed solar cell thin films and nanogratings thickness calculated as 339 nm as tabulated (Table 1) and distance between the triangular gratings 20 nm (10+10 nm). Overall, the proposed ultrathin amorphous silicon solar cell thickness 359 nm.

3. Results and Discussion

In this section, we discuss the influence of front-ITO and rear-Ag triangular nanogratings for the better photovoltaic performance (Figure 2). For the simplicity, first simple guidelines for the designing solar cell integrated in front with the non-dispersive materials of ITO and amorphous silicon. Further, we consider the dispersive Ag rear structure incorporated.

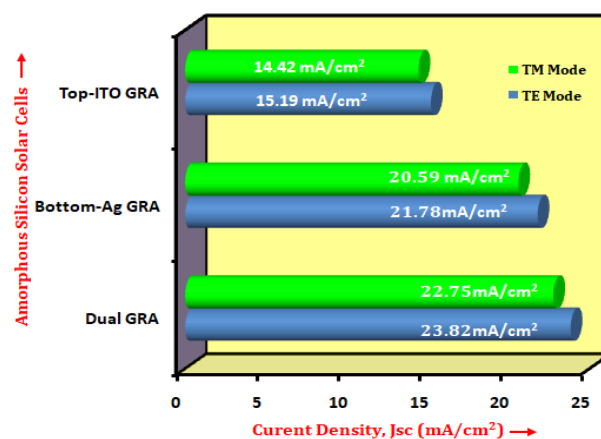


Fig. 2 The current density of ultrathin amorphous silicon solar cells in both polarization modes (TE/TM).

Initially, the ITO anti-reflection coating, amorphous silicon (a-Si) absorber, top-ITO gratings (Top GRA) and Ag substrate integrated solar cell (Top-ITO GRA). This solar cell has achieved current density (J_{sc}) up to 15.19 and 14.42 mA/cm² under transverse electric (TE) and magnetic (TM) fields. In the similar way, instead of top-ITO gratings, the bottom metallic-Ag triangular nanogratings were added. This design solar cell named as “Bottom-Ag GRA”. Here, the dispersive metallic backside reflector is supported and enhanced the collection of the charge carriers (e^- and h^+) by prolonging the photon path length due to the omnidirectional scattering. With this mechanism, the current density further improved up to 20.59 (TM) and 21.78 mA/cm² (TE). Finally, the both top and bottom gratings were added with ARC (ITO), absorber (a-Si) and substrate (Ag). This proposed ultrathin amorphous silicon solar cell (Dual GRA) significantly achieved highest current density of 22.75 (TM) and 23.82 (TE). These comparisons are shown in a bar diagram (Figure 2). Generally, thin film solar cells have weak absorption in the active region due to their effective path length diminishes with the effect of thin geometry for example microscale (1-10 μ m) (Barman *et al.*, 2015). This issue overcomes by addition of suitable nanostructure in thin film solar cell such as triangular nanogratings, dual gratings, and nanoparticles.

Light scattering and diffractions are the most promising light trapping scheme in the thin film amorphous silicon solar cells. The broadband light absorption improvement was noticed from the front rectangular dielectric gratings and back triangular nanogratings combined solar cell structure. Figure 3 (a)-(b) explores light absorption of the various ultrathin amorphous silicon solar cells in both transverse electric (TE) and magnetic (TM) filed. For the comparison, we have included the entire incident solar spectrum. In TE case, the dual gratings (Dual GRA) integrated solar cell shows broader absorption spectra, as compared to the single (top or bottom) grating based cell structure. Consequently, the light absorption furthermore enhanced in TM polarization modes due to the enhanced light scattering on the plasmonic (Ag) nanostructures. The broadband light absorption was noticed from 400-700 nm (λ) by dual grating based ultrathin amorphous silicon solar cells. Using equation (2), the total absorption calculated as shown in Table 2. The total absorption enhanced up to 45.33% in TE mode due to the dual grating nanostructures.

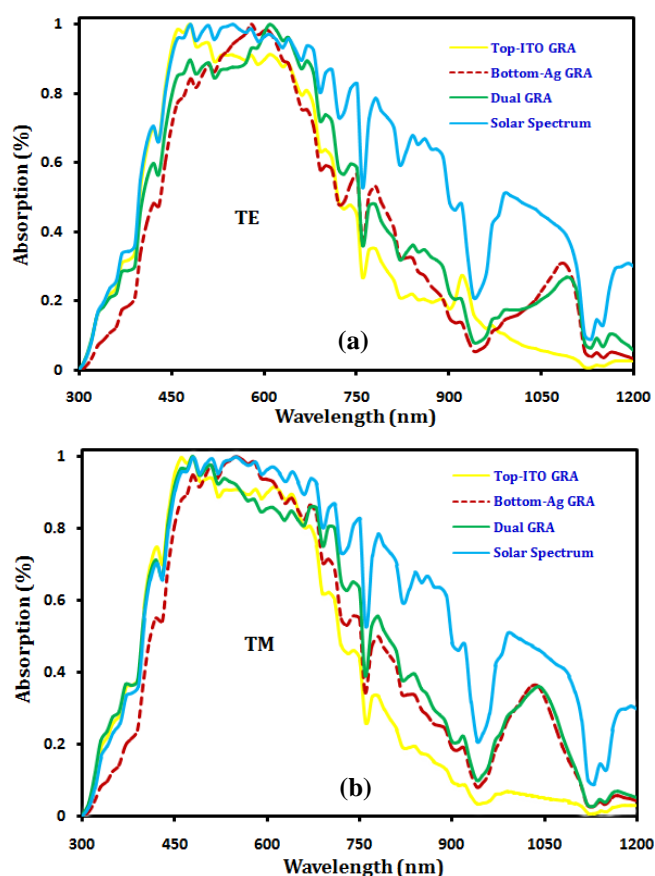


Fig. 3 The absorption spectrum of amorphous silicon solar cells in TE (a) and TM mode (b).

Table 2

The list of total absorption of the various thin film amorphous silicon solar cells

Cell Structure	TE Mode (%)	TM Mode (%)
Top-ITO GRA	31.01	30.25
Bottom-Ag GRA	41.36	39.03
Dual GRA	45.33	43.45
Solar Spectrum	74.25	74.25

Here, the photonic and plasmonic modes plays crucial role for the collection of the light photons by reflection, scattering and transmission such as Fabry-Perot resonance, surface plasmon polariton, surface guided modes, etc. However, the incident solar spectrum highest absorption reached up to 74.25%.

In TM case enhanced absorption noticed due to the surface plasmon resonances and collecting the oscillations of free electrons from the confined surfaces between the metallic and dielectric layers which are strongly interacting with the light (Xia *et al.*, 2013; Zia *et al.*, 2004; Homola *et al.*, 1999).

The photonic and plasmonic effects are evidenced in Figure 4 (a1-a12) and 4(b1-b16) as light (field) distribution. The metallic nanostructures are strongly scattering and reflect the incidence light towards the active region, which helps to inducing the plasmonic modes.

The plasmonic nanostructures can support the localized surface plasmon resonances which are the collective oscillation of the conducting electrons. Furthermore, the physics of the highest absorption peaks of ultrathin amorphous silicon solar cells are explored by electromagnetic theory (Maxwell's equations) (Isabella *et al.*, 2018; Vismara *et al.*, 2019). The spectral peaks are corresponding to the surface, guided modes, Fabry-Perot resonance, Floquet mode, surface plasmon resonance, constructively interfere between the metallic and semiconductors. The primary peaks of the various responsible for the quadruple resonance. The simulated transverse electric (TE) field distribution is shown in Figure 4 (a1)-(a6). It can be clearly observed that the field intensity (red) high near the antireflection coating layer of ITO with the incident wavelength of 509 nm (λ_c). The incident light propagates in the 'Z' direction, while boundaries are set to PBC and PML (Xia *et al.*, 2013). But surface guided mode, Floquet mode, and Fabry-Perot resonance modes are generated within the amorphous silicon absorber region as shows in figure 4(a1).

The low intensity color (pink) appeared at the back of the reflector and it indicates the enhanced absorption. Next, the incident light wavelength (λ_c) increased as 640 nm (figure 4(a2)) and observed strong guiding modes (cyan) started at the tip of the bottom triangular gratings and between the gratings. This phenomenon is known as surface excitation between the metallic and dielectric surfaces. With the continuation of surface guided modes (cyan color), further extended into the amorphous silicon absorber region as depicted in figure 4 (a3). Between the nanogratings of ITO and Ag, the strong field (green color) appeared within the absorber region (Raghvendra Sarvjeet Dubey and Sigamani, 2014). At 769 nm (λ_c), the strong field further extended and appeared in the red color as shows in figure 4(a4). Figure 4(a5) -(a6), depicts the strong field between the gratings ($\lambda_c=780$ nm) and reduced at 840 nm incident wavelength. Since, many decades the low light absorption appeared at 840 nm and this is a major issue with the solar cells which is to be optimized. The incidence wavelength of 919 nm (Figure 4(a7)) generated the surface guided modes at the bottom of the metal gratings and increased the light absorption in the absorber region due to that sharp peak appeared in Figure 3(a).

Figure 4(a8)-(a9) shows the strong field between the metallic and dielectric gratings (λ_c , 968 & 990 nm) and low field distribution noticed from 1100, 1170 and 1200 nm compared to the ultraviolet spectral region as shown in Figure 4(a10)-(a12). Overall, the tapering nanostructure allows strong and smooth electric transition with Fabry-Perot modes appeared due to the traditional structure. Figure 4 (b1) shows (429 nm) the strong light intensity at the top of the anti-reflection coating (ARC) and started to spread light into the absorber region due to that surface guided modes generated at the bottom of the ARC layer. First, the incident light of 460 nm, the light reached into the bottom of the triangular gratings with the guided modes as depicted in Figure 4(b2). Next, the light (509 nm) reached at the bottom of the gratings a solid line (Figure 4(b3)) and localized surface plasmon, LSP (red colour, 530 nm) started at the top of the silver gratings as shown in Figure 4(b4). These surface plasmon resonances of a nanostructure are affected by the size, shape and semiconductor materials (Barman *et al.*, 2015).

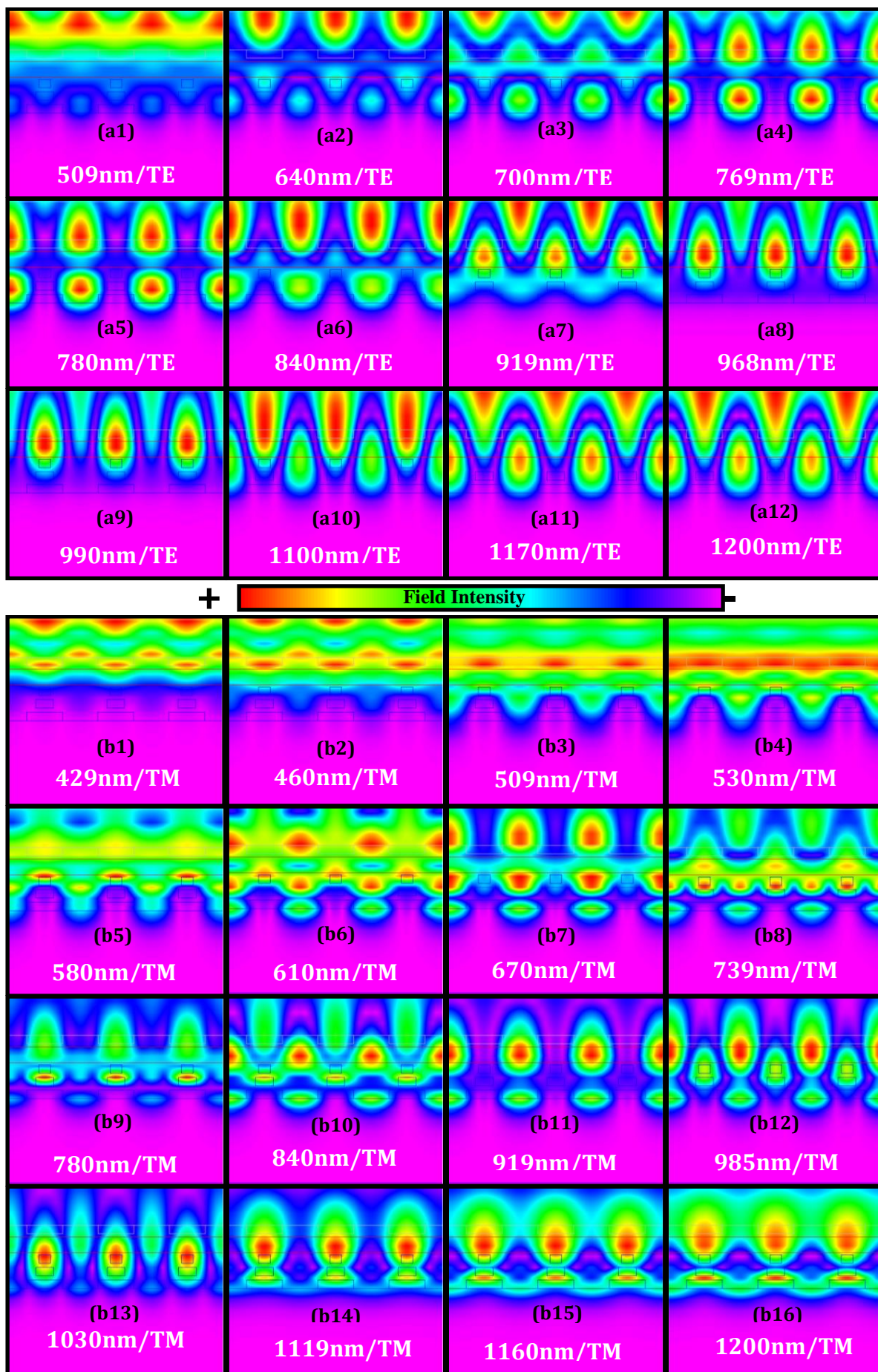


Fig. 4 Field distribution at different wavelengths in TE (a1)-(a12) and TM (b1)-(b16).

From the Figure 4(b1) - (b4) shows wavelike nature and light distribution clear to reach the entire solar cell. Furthermore, the light intensity, enhanced from 580 to 739 nm incidence wavelength. Figure 4(b5) represents the strong LSP on the silver gratings and again increased light distribution between the gratings and absorber. The surface plasmon modes, guided modes, LSP and surface excitation noticed from 610 to 919 nm (Figure 4(b6)-(b11)). Here, the surface plasmon resonance is tuned by metallic structure, size, shape and thickness. The optimal plasmonic (Ag) nanostructure could generate the improved absorption spectrum in order to further enhance incidence light harvesting capability (Saravanan and Dubey, 2016; Prabhakar rai, 2019). At 985 nm wavelength, the reduced localized light on the gratings and excitation of field between metal and dielectric interfaces as shows in Figure 4(b12). The infrared spectral region (>1000 nm) localized field intensity, enhanced in the absorber region as depicted in the Figure 4(b13m)-(b14) and reduced the collection of charge carriers due to thermal losses and unabsorbed photons (Joseph *et al.*, 2019; Sha *et al.*, 2010). Figure 4(b14) shows the strong LSPR modes and further enhanced the optical efficiency and reduced the field intensity at 1160 and 1200 nm. However, the field intensity or LSP enhanced in between the triangular gratings as depicted in Figure 4(b15)-(b16). Overall, the influence of plasmonic nanostructure the photon absorption enhanced in the absorber region with the help of strong light scattering as shown in Figure 3(b).

6. Conclusion

In conclusion, we have demonstrated the possibility of highest current density in ultrathin film amorphous silicon solar cells by incorporating front-ITO and rear-Ag nanogratings. These ultrathin film amorphous silicon solar cell investigations were carried out by using rigorous coupled wave analysis (RCWA) method. The detailed comparison made between single and dual nanogratings integrated ultrathin film plasmonic solar cell for better optical performances and found later one structure yielded a substantial photocurrent increased from 15.19 to ~23 mA/cm² (TE mode). Moreover, the dual grating nanostructure plays crucial role for the enhancement of the current density by larger angle scattering and diffraction mechanism due to that noticed an additional absorption in the longer spectral region. These light trapping mechanisms were evidenced by the field distributions (TE/TM) at various center wavelengths. Furthermore, the results provide a theoretical investigation and technical support for the fabrication and optimization of the ultrathin film amorphous silicon solar cells.

Author Contributions: R.S. Dubey: Conceptualization, methodology, S. Saravanan: Supervision, resources, project administration, writing—review and editing, project administration, validation, writing—review and editing, project administration, formal analysis, writing—original draft, validation. All authors have read and agreed to the published version of the manuscript.

Funding: The author(s) received no financial support for the research, authorship, and/or publication of this article.

Conflicts of Interest: The authors declare no conflict of interest.

References

- Agrawal, M. and Peumans, P. (2008). Broadband optical absorption enhancement through coherent light trapping in thin-film photovoltaic cells. *Opt. Express*, 16(8), 5385–5396. <https://doi.org/10.1364/OE.16.005385>
- Barman, B., Chaudhary, S., Verma, A., Jain, V.K. (2015). Study of formation and influence of surface plasmonic silver nanoparticles in efficiency enhancement for c-Si solar cells. *AIP Conf. Proc.*, 1731, 050142-1-3. DOI: 10.1063/1.4947796
- Belhadji, Y. (2022). Numerical modelling of CuInxGa(1-x)Se₂/WS₂ thin solar cell with an enhanced PCE. *Int. J. Renew. Energy Dev.*, 11(2), 393-401. <https://doi.org/10.14710/ijred.2022.38527>
- Catchpole, K.R. and Polman, A., (2008). Plasmonic solar cells. *Optics Express*, 16(26), 21793-21800. <https://doi.org/10.1364/OE.16.021793>
- Chen, X., Jia, B., Saha, J.K., Cai, B., Stokes, N., Qiao, Q., Wang, Y., Shi, Z., Gu, M., (2012). Broadband enhancement in thin-film amorphous silicon solar cells enabled by nucleated silver nanoparticles. *Nano Lett.*, 12(5), 2187-2192. <https://doi.org/10.1021/nl203463z>
- Chriki, R., Yanai, A., Shappir, J., Levy, U. (2013). Enhanced efficiency of thin film solar cells using a shifted dual grating plasmonic structure. *Opt. Express*, 21 (S3), A382-A391. <https://doi.org/10.1364/OE.21.00A382>
- Dubey, R.S. and Sigamani, S. (2014). Performance evaluation of thin film silicon solar cell based on dual diffraction grating. *Nanoscale Res. Lett.*, 9, 688. <https://doi.org/10.1186/1556-276X-9-688>
- Gong, C. and Leite, M.S. (2016). Noble metal alloys for plasmonics. *ACS Photonics*, 3(4), 507-513. DOI: 10.1021/acsp Photonics.5b00586
- Hamdani, D., Prayogi, S., Cahyono, Y., Yudoyono, G., Darminto, D. (2022). The effects of dopant concentration on the performance of the a-SiOx:H(p)/a-Si:H(i1)/a-Si:H(n) heterojunction solar cell. *Int. J. Renew. Energy Dev.*, 11(1), 173-181. <https://doi.org/10.14710/ijred.2022.40193>
- Homola, J., Yee, S.S., Gauglitz, G. (1999). Surface plasmon resonance sensors: Review. *Sens. Actuator B.*, 54, 3-15. [https://doi.org/10.1016/S0925-4005\(98\)00321-9](https://doi.org/10.1016/S0925-4005(98)00321-9)
- Isabella, O., Vismara, R., Linszen, D.N.P., Wang, K.X., Fan, S., Zeman, M. (2018). Advanced light trapping scheme in decoupled front and rear textured thin-film silicon solar cells. *Sol. Energy*, 162(5), 344. <https://doi.org/10.1016/j.solener.2018.01.040>
- Joseph, D., Senthilarasu, S., Mallick, T.K. (2019). Improving spectral modification for applications in solar cells: A review. *Renewable Energy*, 132, 186-205. <https://doi.org/10.1016/j.renene.2018.07.101>
- Khai Q.L., Abass, A., Maes, B., Bienstman, P., Alu A. (2011). Comparing plasmonic and dielectric gratings for absorption enhancement in thin-film organic solar cells. *Opt. Express*, A39-A50. <https://doi.org/10.1364/OE.20.000A39>
- Meng X., Drouard E., Gomard G., Peretti R., Fave A., Seassal, C. (2012). Combined front and back diffraction gratings for broad band light trapping in thin film solar cell. *Opt. Express*, A560-571. <https://doi.org/10.1364/OE.20.00A560>
- Phengdaam A., Nootchanat, S., Ishikawa, R., Lertvachirapaiboon, C., Kato, K., Sanong, E., Baba, A. (2021). Improvement of organic solar cell performance by multiple plasmonic excitations using mixed-silver nanoprisms. *Journal of Science: Advanced Materials and Devices*, 6, 264-270. <https://doi.org/10.1016/j.jsamd.2021.02.007>
- Pillai, S. and Green, M.A. (2010). Plasmonic for photovoltaic applications. *Sol. Energy Mater. Sol. Cells*, 94 (9), 1481-1486. <https://doi.org/10.1016/j.solmat.2010.02.046>
- Prabhakar, R. (2019). Plasmonic noble metal-metal oxide core-shell nanoparticles for dye-sensitized solar cell applications. *Sustainable Energy Fuels*, 3, 63-91. DOI: 10.1039/C8SE00336J
- Saadim, F., Forhad, T., Sikder, A., Ghann, W., Ali, M.M., Sither, V., Ahammad, A.J. S, Subhan Md. A., Uddin, J. (2020). Enhancing the performance of dye sensitized solar

- cells using silver nanoparticles modified photoanode. *Molecules*, 25, 4021-1-10. doi:10.3390/molecules25174021
- Saravanan, S. and Dubey, R.S., (2015). Design and analysis of thin film silicon solar cells using FDTD method, *Procedia Materials Science*, 10, 301-306. <https://doi.org/10.1016/j.mspro.2015.06.054>
- Saravanan, S. and Dubey, R.S., (2021). Study of ultrathin-film amorphous silicon solar cell performance using photonic and plasmonic nanostructure. *Int. J. Energy Res.* 46(3), 2558-2566. <https://doi.org/10.1002/er.7328>
- Saravanan, S. and Dubey, R.S., (2016). Optical absorption in 40 nm ultrathin film silicon solar cells assisted by photonic and plasmonic modes. *Opt. Commun.*, 377, 65-69. <https://doi.org/10.1016/j.optcom.2016.05.028>
- Schuller, J.A., Barnard, E.S., Cai, W., Jun, Y.C., White, J.S., Brongersma, M.L. (2010). Plasmonics for extreme light concentration and manipulation. *Nature Materials*, 9, 193-204. <https://doi.org/10.1038/nmat2630>
- Sha, W.E.I., Choy, W.C.H., Chew, W.C. (2010). A comprehensive study for the plasmonic thin-film solar cell with periodic structure. *Opt. Express*, 18 (6), 5993-6007. <https://doi.org/10.1364/OE.18.005993>
- Shi, Y., Wang, X., Liu, W., Yang, T., Xu, R., Yang, F. (2013). Multilayer silver nanoparticles for light trapping in thin film solar cells. *J. Appl. Phys*, 113, 176101-1-4. <https://doi.org/10.1063/1.4803676>
- Singh, G. and Verma, S.S. (2017). Enhanced efficiency of thin film GaAs solar cells with plasmonic metal nanoparticles. *Energy Sources, Part A: Recovery, Utilization, and Environmental Effects*, 1-9. <https://doi.org/10.1080/15567036.2017.1407840>
- Tran, V.T., Nguyen, H.Q., Kim, Y.M., Ok, G., Lee, J. (2020). Photonic-plasmonic nanostructures for solar energy utilization and emerging biosensors. *Nanomaterials*. 10, 2248-1-19. <https://doi.org/10.3390/nano10112248>
- Vismara, R., Lank, N.O., Verre, R., Kall, M., Isabella, O., Zeman, M. (2019). Solar harvesting based on perfect absorbing all-dielectric nanoresonators on a mirror. *Opt. Express*, 27 (16), A967-A980. <https://doi.org/10.1364/OE.27.00A967>
- Xia, Z., Wu, Y., Liu, R., Tang, P., Liang, Z., (2013). Light trapping enhancement with combined front metal nanoparticles and back diffraction gratings. *Chinese Optics Letters*, 11, S10503-1-4. DOI: 10.3788/COL201311.S10503
- Zia, R., Selker M.D., Catrysse P.B., Brongersma M.L., (2004). Geometries and materials for subwavelength surface plasmon modes. *J. Opt. Soc. Am. A*, 21, 2442-2446. DOI:10.1364/JOSAA.21.002442



© 2022. The Author(s). This article is an open access article distributed under the terms and conditions of the Creative Commons Attribution-ShareAlike 4.0 (CC BY-SA) International License (<http://creativecommons.org/licenses/by-sa/4.0/>)